STATE OF THE CLIMATE IN 2023

THE TROPICS

H. J. Diamond and C. J. Schreck, Eds.

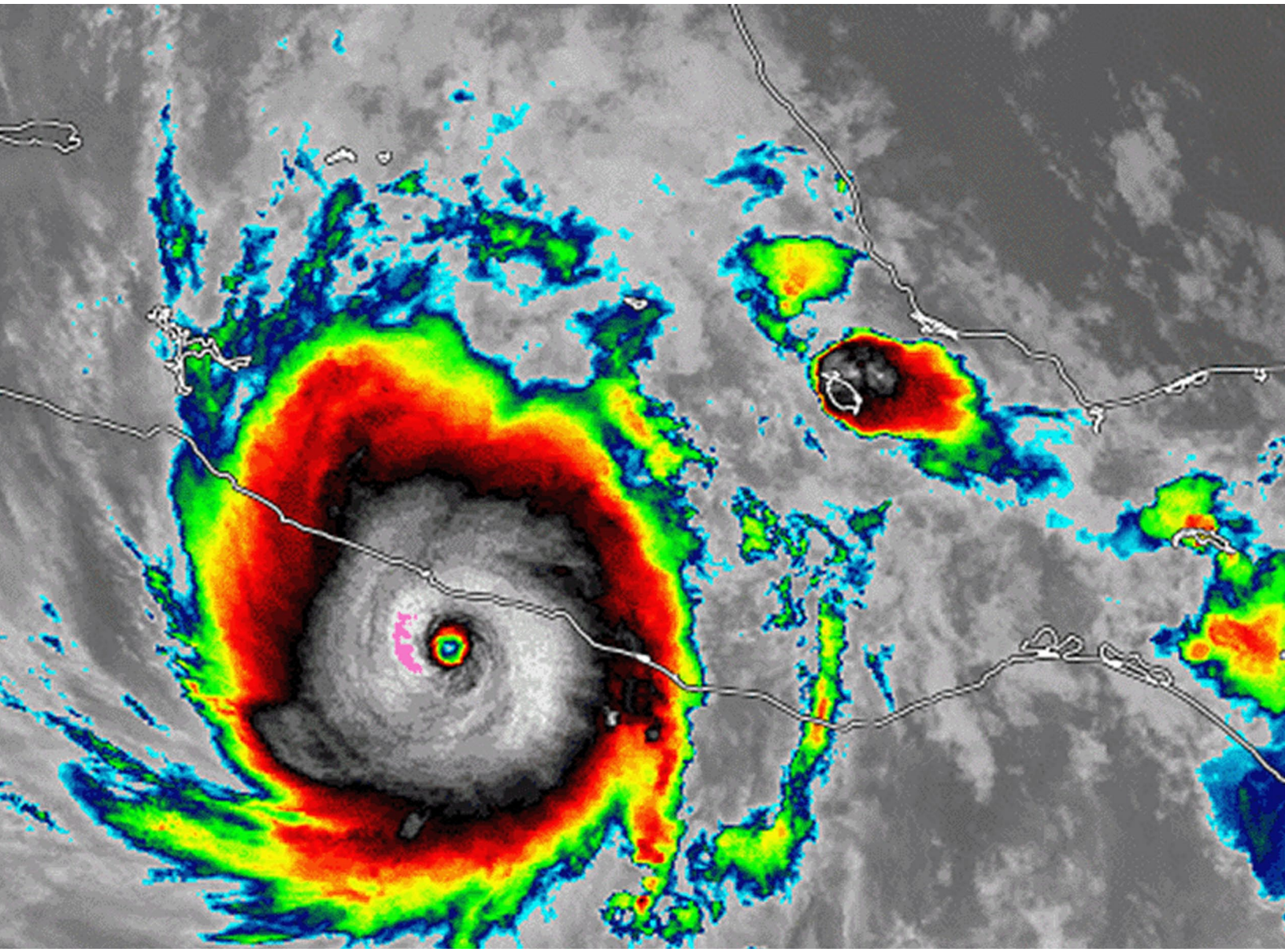

Special Online Supplement to the *Bulletin of the American Meteorological Society*, Vol. 105, No. 8, August 2024

https://doi.org/10.1175/BAMS-D-24-0098.1

Corresponding author: Howard J. Diamond / howard.diamond@noaa.gov

©2024 American Meteorological Society
For information regarding reuse of this content and general copyright information, consult the AMS Copyright Policy.

STATE OF THE CLIMATE IN 2023
The Tropics

Editors

Jessica Blunden
Tim Boyer

Chapter Editors

Anthony Arguez
Josh Blannin
Peter Bissolli
Kyle R. Clem
Howard J. Diamond
Matthew L. Druckenmiller
Robert J. H. Dunn
Catherine Ganter
Nadine Gobron
Gregory C. Johnson
Rick Lumpkin
Rodney Martinez
Ademe Mekonnen
John B. Miller
Twila A. Moon
Marilyn N. Raphael
Carl J. Schreck III
Laura Stevens
Richard L. Thoman
Kate M. Willett
Zhiwei Zhu

Technical Editor

Lukas Noguchi

BAMS Special Editor for Climate

Timothy DelSole

American Meteorological Society

Cover Credit:
Hurricane Otis 25 October 2023

Hurricane Otis experienced extremely rapid intensification in the 12 hours before it made landfall near Acapulco, Mexico, as a Category 5 storm on 25 October 2023.

Imagery courtesy of CIMSS - Cooperative Institute for Meteorological Satellite Studies, University of Wisconsin-Madison

How to cite this document:
The Tropics is one chapter from the *State of the Climate in 2023* annual report and is available from https://doi.org/10.1175/BAMS-D-24-0098.1. Compiled by NOAA's National Centers for Environmental Information, *State of the Climate in 2023* is based on contributions from scientists from around the world. It provides a detailed update on global climate indicators, notable weather events, and other data collected by environmental monitoring stations and instruments located on land, water, ice, and in space. The full report is available from https://doi.org/10.1175/2024BAMSStateoftheClimate.1.

Citing the complete report:
Blunden, J. and T. Boyer, Eds., 2024: "State of the Climate in 2023". *Bull. Amer. Meteor. Soc.*, **105** (8), Si–S483 https://doi.org/10.1175/2024BAMSStateoftheClimate.1.

Citing this chapter:
Diamond, H.J. and C. J. Schreck, Eds., 2024: The Tropics [in "State of the Climate in 2023"]. *Bull. Amer. Meteor. Soc.*, **105** (8), S214–S276, https://doi.org/10.1175/BAMS-D-24-0098.1.

Citing a section (example):
Klotzbach, P., C. Fogarty, and R. Truchelut, 2024: Hurricane Otis: The strongest landfalling hurricane on record for the west coast of Mexico [in "State of the Climate in 2023"]. *Bull. Amer. Meteor. Soc.*, **105** (8), S264–S265, https://doi.org/10.1175/BAMS-D-24-0098.1.

Editor and Author Affiliations (alphabetical by name)

Allgood, Adam, NOAA/NWS National Centers for Environmental Prediction Climate Prediction Center, College Park, Maryland

Becker, Emily J., Rosenstiel School of Marine and Atmospheric Science, University of Miami, Miami, Florida

Blake, Eric S., NOAA/NWS National Hurricane Center, Miami, Florida

Bringas, Francis G., NOAA/OAR Atlantic Oceanographic and Meteorological Laboratory, Miami, Florida

Camargo, Suzana J., Lamont-Doherty Earth Observatory, Columbia University, Palisades, New York

Cerveny, Randall, Department of Geography, Arizona State University, Tempe, Arizona

Chen, Lin, Institute for Climate and Application Research (ICAR)/KLME/ILCEC/CIC-FEMD, Nanjing University of Information Science and Technology, Nanjing, China

Coelho, Caio A.S., Centro de Previsão do Tempo e Estudos Climáticos/National Institute for Space Research, Center for Weather Forecasts and Climate Studies, Cachoeira Paulista, Brazil

Diamond, Howard J., NOAA/OAR Air Resources Laboratory, College Park, Maryland

Earl-Spurr, Craig, Bureau of Meteorology, Perth, Australia

Fauchereau, Nicolas, National Institute of Water and Atmospheric Research, Ltd., Auckland, New Zealand

Fogarty, Chris, Canadian Hurricane Centre, Dartmouth, Canada

Goldenberg, Stanley B., NOAA/OAR Atlantic Oceanographic and Meteorological Laboratory, Miami, Florida

Harnos, Daniel S., NOAA/NWS National Centers for Environmental Prediction Climate Prediction Center, College Park, Maryland

He, Qiong, Earth System Modeling Center, Nanjing University of Information Science and Technology, Nanjing, China

Hu, Zeng-Zhen, NOAA/NWS National Centers for Environmental Prediction Climate Prediction Center, College Park, Maryland

Klotzbach, Philip J., Department of Atmospheric Science, Colorado State University, Fort Collins, Colorado

Knaff, John A., NOAA/NESDIS Center for Satellite Applications and Research, Fort Collins, Colorado

Kumar, Arun, NOAA/NWS National Centers for Environmental Prediction Climate Prediction Center, College Park, Maryland

L'Heureux, Michelle, NOAA/NWS National Centers for Environmental Prediction Climate Prediction Center, College Park, Maryland

Landsea, Chris W., NOAA/NWS National Hurricane Center, Miami, Florida

Lin, I-I, National Taiwan University, Taipei, Taiwan

Lopez, Hosmay, NOAA/OAR Atlantic Oceanographic and Meteorological Laboratory, Miami, Florida

Lorrey, Andrew M., National Institute of Water and Atmospheric Research, Ltd., Auckland, New Zealand

Luo, Jing-Jia, Institute for Climate and Application Research, Nanjing University of Information Science and Technology, Nanjing, China

Magee, Andrew D., Centre for Water, Climate and Land, School of Environmental and Life Sciences, University of Newcastle, Callaghan, Australia

Pasch, Richard J., NOAA/NWS National Hurricane Center, Miami, Florida

Paterson, Linda, Bureau of Meteorology, Perth, Australia

Pezza, Alexandre B., Greater Wellington Regional Council, Wellington, New Zealand

Rosencrans, Matthew, NOAA/NWS National Centers for Environmental Prediction Climate Prediction Center, College Park, Maryland

Schreck, Carl J., Cooperative Institute for Satellite Earth System Studies, North Carolina State University, Asheville, North Carolina

Trewin, Blair C., Bureau of Meteorology, Melbourne, Australia

Truchelut, Ryan E., WeatherTiger, Tallahassee, Florida

Uehling, John, Cooperative Institute for Satellite Earth System Studies, North Carolina State University, Asheville, North Carolina

Wang, Bin, School of Ocean and Earth Science and Technology, Department of Meteorology, University of Hawaii at Manoa, Honolulu, Hawaii; International Pacific Research Center, Honolulu, Hawaii

Wang, Hui, NOAA/NWS National Centers for Environmental Prediction Climate Prediction Center, College Park, Maryland

Wood, Kimberly M., Department of Hydrology and Atmospheric Sciences, University of Arizona, Tucson, Arizona

Editorial and Production Team

Allen, Jessicca, Graphics Support, Cooperative Institute for Satellite Earth System Studies, North Carolina State University, Asheville, North Carolina

Camper, Amy V., Graphics Support, Innovative Consulting and Management Services, LLC, NOAA/NESDIS National Centers for Environmental Information, Asheville, North Carolina

Haley, Bridgette O., Graphics Support, NOAA/NESDIS National Centers for Environmental Information, Asheville, North Carolina

Hammer, Gregory, Content Team Lead, Communications and Outreach, NOAA/NESDIS National Centers for Environmental Information, Asheville, North Carolina

Love-Brotak, S. Elizabeth, Lead Graphics Production, NOAA/NESDIS National Centers for Environmental Information, Asheville, North Carolina

Ohlmann, Laura, Technical Editor, Innovative Consulting and Management Services, LLC, NOAA/NESDIS National Centers for Environmental Information, Asheville, North Carolina

Noguchi, Lukas, Technical Editor, Innovative Consulting and Management Services, LLC, NOAA/NESDIS National Centers for Environmental Information, Asheville, North Carolina

Riddle, Deborah B., Graphics Support, NOAA/NESDIS National Centers for Environmental Information, Asheville, North Carolina

Veasey, Sara W., Visual Communications Team Lead, Communications and Outreach, NOAA/NESDIS National Centers for Environmental Information, Asheville, North Carolina

h. Tropical cyclone heat potential

—F. Bringas, I-I. Lin, and J. A. Knaff

Tropical cyclone heat potential (TCHP) is an indicator of the amount of heat stored in the upper ocean that can potentially promote tropical cyclone (TC) intensification and regulate ocean–atmosphere enthalpy fluxes and TC-induced sea-surface temperature (SST) cooling (e.g., Lin et al. 2013). TCHP is calculated by integrating the ocean temperature between the sea surface and the 26°C isotherm (D26), which has been reported as the minimum temperature required for TC genesis and intensification (Leipper and Volgenau 1972; Dare and McBride 2011). TCs traveling over regions of high TCHP conditions experience higher heat fluxes from the ocean into the atmosphere, favoring intensification and leading to reduced SST cooling (e.g., Lin et al. 2013). Areas in the ocean with TCHP values above 50 kJ cm^{-2} have been statistically linked with TC intensification, including rapid intensification when the maximum sustained wind speed increases by at least 30 kt in 24 hours in situations in which atmospheric conditions are favorable (e.g., Shay et al. 2000; Mainelli et al. 2008; Lin et al. 2021; Knaff et al. 2018, 2020). In addition to upper-ocean heat content, upper-ocean salinity conditions may also modulate TC intensification as storms traveling over areas of fresh water-induced barrier layers may receive increased air–sea heat fluxes caused by reduced upper-ocean mixing and cooling (e.g., Balaguru et al. 2012; Domingues et al. 2015).

We present an assessment and analysis of the upper-ocean heat content conditions during 2023, based on estimates of two parameters: 1) TCHP (e.g., Goni et al. 2009, 2017) global anomalies with respect to their long-term mean (1993–2022) and 2) TCHP in 2023 compared to conditions observed in 2022. TCHP anomalies during 2023 (Fig. 4.40) are computed for June–November in the Northern Hemisphere and November 2022–April 2023 in the Southern Hemisphere. The seven regions where TCs typically form, travel, and weaken/intensify are highlighted in Fig. 4.40. In all these regions, TCHP values exhibit large temporal and spatial variability due to mesoscale features (e.g., surface currents and associated eddies and rings) and short- to long-term modes of climate variability (e.g., North Atlantic Oscillation, El Niño–Southern Oscillation, and the Pacific Decadal Oscillation). The differences in TCHP anomalies between 2023 and 2022, as depicted in Fig. 4.41, were computed for the primary months of TC activity in each hemisphere as described above.

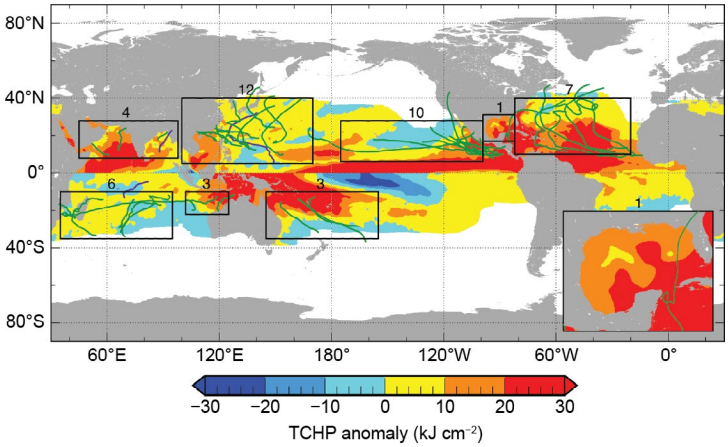

Fig. 4.40. Global anomalies of tropical cyclone heat potential (TCHP; kJ cm^{-2}) during 2023 computed as described in the text. The boxes indicate the seven regions where TCs typically occur; from left to right: southwest Indian, North Indian, northwest Pacific, southeast Indian, South Pacific, northeast Pacific, and North Atlantic (shown as Gulf of Mexico and tropical Atlantic separately). The green lines indicate the trajectories of all tropical cyclones reaching at least Category 1 (1-minute average wind ≥64 kt) and above during Nov 2022–Apr 2023 in the Southern Hemisphere and Jun–Nov 2023 in the Northern Hemisphere, and purple lines indicate Category 1 TCs that occurred outside these periods. The number above each box corresponds to the number of Category 1 and above cyclones that traveled within that box. Gulf of Mexico is shown in the inset in the lower right corner.

TCHP anomalies during 2023 exhibited above-average values in all TC regions and basins, including the eastern North Pacific and western North Pacific and the southwest Indian Ocean where, despite smaller areas of negative anomalies, average values in the regions were positive albeit closer to the long-term mean (Fig. 4.40). These positive TCHP anomalies were particularly large in most areas of the North Indian, the southwest Pacific, the North Atlantic, the Gulf of Mexico, and the equatorial regions of the eastern North Pacific where most TCs travel and intensify. TCHP anomalies reached values up to 30 kJ cm^{-2}, which are indicative of favorable oceanic conditions for the development and intensification of TCs. These same regions had TCHP anomalies during 2023 that were more than 20 kJ cm^{-2} larger than in 2023. Meanwhile, the South Indian Ocean, the western North Pacific, and the Bay of Bengal had near- or below-average

TCHP anomalies during 2023, and their TCHP was lower in 2023 compared to the previous year (Fig. 4.41).

The positive anomalies in the eastern North Pacific and central Pacific equatorial areas, with values during 2023 larger than 50 kJ cm^{-2} compared to 2022 (Fig. 4.41), were associated with the El Niño. In contrast, over the western North Pacific, negative anomalies of –10 kJ cm^{-2} to –20 kJ cm^{-2} as compared to 2022 were observed, consistent with a strong El Niño, which is known to reduce TCHP in the northwest Pacific (Zheng et al. 2015; Lin et al. 2020).

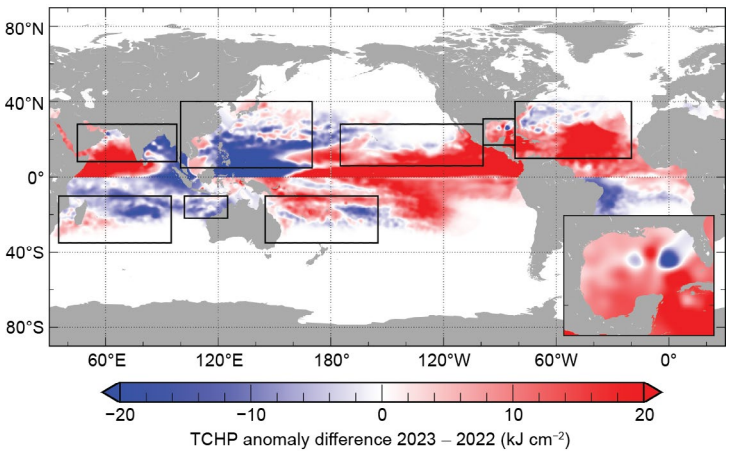

Fig. 4.41. Tropical cyclone heat potential (TCHP) anomaly difference between the 2023 and 2022 tropical cyclone seasons (kJ cm^{-2}; Jun–Nov in the Northern Hemisphere and Nov–Apr in the Southern Hemisphere). The Gulf of Mexico is shown in the inset in the lower right corner.

Consistent with the observed slightly above-average TCHP anomalies during 2023 in the region, the 2022/23 southwest Indian Ocean cyclone season was below average in terms of named storms but above average in terms of accumulated cyclone energy (ACE; Fig. 4.40). The most intense storm of the season was Cyclone Freddy. During its westward track until making landfall in Madagascar and Mozambique, Freddy weakened and re-intensified repeatedly, completing seven independent cycles of rapid intensification while traveling over areas with SSTs greater than 28°C and a TCHP greater than 40 kJ cm^{-2} (see Sidebar 4.2 for details).

Large positive areas of high TCHP anomaly values, in excess of 30 kJ cm^{-2} from the long-term average, were observed in regions of the southwest Indian and southwest Pacific, where TCs typically form and develop. However, 2022/23 generated near-average TC activity in these regions with a total of six TCs, of which four reached Category 1 intensity or above.

In the North Indian Ocean, above-average TCHP anomalies in excess of 30 kJ cm^{-2} and 10 kJ cm^{-2} were observed during 2023 in the northern Arabian Sea and the southern Bay of Bengal, respectively (Fig. 4.40). The most intense storm was Category 5 TC Mocha, which occurred in May (Fig. 4.40, in purple). After being named in the Bay of Bengal on 9 May, Mocha experienced two cycles of rapid intensification on 12 May and then 13 May, reaching its estimated peak intensity of 1-minute sustained wind speed of 140 kt (72 m s^{-1}) and a minimum central barometric pressure of 918 hPa, according to the Joint Typhoon Warning Center (JTWC), while traveling over extremely favorable oceanic conditions characterized by SSTs greater than 30°C and a TCHP greater than 120 kJ cm^{-2}.

Upper-ocean thermal conditions are largely modulated by the state of the El Niño–Southern Oscillation (ENSO) in the North Pacific Ocean (e.g., Zheng et al. 2015; Lin et al. 2020). While La Niña was predominant in the region during 2022, a shift to El Niño started early in 2023 with the transition occurring by June. El Niño became strong by late 2023 (section 4b). Consistent with this change in the ENSO state, TCHP anomalies were positive in the equatorial region of the eastern North Pacific with values well above 30 kJ cm^{-2}, while in the western North Pacific TCHP anomalies were positive although closer to the long-term mean (Fig. 4.40). Compared to 2022, TCHP anomalies in the eastern North Pacific during 2023 were larger by more than 20 kJ cm^{-2} in the equatorial regions while they were mostly negative by a similar magnitude in the western North Pacific (Fig. 4.41).

Tropical cyclone activity in the western North Pacific in 2023 was relatively low, although seven TCs reached Category 4 or 5 status. Among them, Super Typhoon Mawar was the most intense TC of the northwest Pacific in 2023, with a maximum intensity of 160 kt (82 m s^{-1}), according to the JTWC. Mawar originated and intensified at relatively low latitudes (~15°N) in May. At this low latitude, even in May, TCHP values were still high (~140 kJ cm^{-2}) and could favor Mawar's intensification.

The favorable oceanic conditions for TC intensification noted in the eastern North Pacific likely contributed to the above-average hurricane season observed during 2023. The two most

intense TCs of the season were Category 5 Hurricanes Jova and Otis, which underwent short periods of rapid intensification while traveling over regions of similar upper ocean thermal conditions characterized by SSTs greater than 29°C and a TCHP greater than 80 kJ cm^{-2}.

In the North Atlantic basin, upper-ocean thermal conditions during the 2023 hurricane season were characterized by TCHP anomalies larger than the long-term average, except in a reduced area near the northeast coast of the United States, where TCHP anomalies were slightly negative with respect to the long-term mean (Fig. 4.40). In particular, large TCHP anomalies were observed in the southeast portion of the basin west of Africa, the Caribbean Sea and the tropical North Atlantic around Cuba, and the Gulf of Mexico, where TCHP anomalies reached average values of up to 35 kJ cm^{-2} during the season. The same spatial distribution was observed for areas of TCHP anomalies that were larger in 2023 compared to the previous year throughout most of the region (Fig. 4.41), with anomalies in excess of 25 kJ cm^{-2} in the areas with the largest TCHP anomalies during 2023. It is likely that these favorable upper ocean thermal conditions contributed to 2023 being the fourth most active on record for named storm formations, with a total of 20 named storms (Fig. 4.40). The 2023 season was also the most active season on record for a year with a strong El Niño; Category 5 Hurricane Lee was the strongest storm of the season in this region. The system traveled over areas of favorable oceanic conditions with SSTs greater than 30°C and a TCHP greater than 90 kJ cm^{-2}, reaching its estimated peak intensity of 145 kt (75 m s^{-1}) and a minimum central barometric pressure of 926 hPa. Lee rapidly intensified from Category 1 to Category 5 during a 24-hour period with an increase in wind speed of 75 kt (39 m s^{-1}). Despite these favorable oceanic conditions, Lee subsequently weakened due to TC-unfavorable atmospheric conditions, including an increase in vertical wind shear.

In summary, favorable upper-ocean thermal conditions were observed in all TCHP basins during the 2023 season, except for the western North Pacific and southeast Indian Ocean, where conditions were slightly above average compared to the long-term mean. TCHP anomalies during 2023 were higher in most basins compared to the previous year, with the exception of the same two regions (western North Pacific and southeast Indian Ocean basins) where anomalies during 2023 were lower than those of the previous year. TC activity based on the number of named storms was consistent with these thermal conditions for every region. Several storms, including Intense Cyclone Freddy in the southwest Indian, Super Typhoon Mawar in the western North Pacific, Major Hurricanes Jova and Otis in the eastern North Pacific, and Major Hurricane Lee in the North Atlantic underwent rapid intensification, including several independent rapid intensification cycles in some cases, while traveling over areas with favorable oceanic conditions with high SST and TCHP values.

References

Aiyyer, A., and J. Molinari, 2008: MJO and tropical cyclogenesis in the Gulf of Mexico and eastern Pacific: Case study and idealized numerical modeling. *J. Atmos. Sci.*, **65**, 2691–2704, https://doi.org/10.1175/2007JAS2348.1.

Aon, 2024: Climate and catastrophe insight report. Aon, 118 pp., https://assets.aon.com/-/media/files/aon/reports/2024/climate-and-catastrophe-insights-report.pdf.

Balaguru, K., P. Chang, R. Saravanan, L. R. Leung, Z. Xu, M. Li, and J. S. Hsieh, 2012: Ocean barrier layers' effect on tropical cyclone intensification. *Proc. Natl. Acad. Sci. USA*, **109**, 14343–14347, https://doi.org/10.1073/pnas.1201364109.

Banzon, V. F., and R. W. Reynolds, 2013: Use of WindSat to extend a microwave-based daily optimum interpolation sea surface temperature time series. *J. Climate*, **26**, 2557–2562, https://doi.org/10.1175/JCLI-D-12-00628.1.

Beck, H. E., E. F. Wood, M. Pan, C. K. Fisher, D. G. Miralles, A. I. J. M. van Dijk, T. R. McVicar, and R. F. Adler, 2019: MSWEP V2 Global 3-hourly 0.1° precipitation: Methodology and quantitative assessment. *Bull. Amer. Meteor. Soc.*, **100**, 473–500, https://doi.org/10.1175/BAMS-D-17-0138.1.

Behringer, D. W., 2007: The Global Ocean Data Assimilation System (GODAS) at NCEP. 11th Symp. on Integrated Observing and Assimilation Systems for Atmosphere, Oceans, and Land Surface, San Antonio, TX, Amer. Meteor. Soc., 3.3, http://ams.confex.com/ams/87ANNUAL/techprogram/paper_119541.htm.

——, M. Ji, and A. Leetmaa, 1998: An improved coupled model for ENSO prediction and implications for ocean initialization. Part I: The ocean data assimilation system. *Mon. Wea. Rev.*, **126**, 1013–1021, https://doi.org/10.1175/1520-0493(1998)126<1013:AICMFE>2.0.CO;2.

Bell, G. D., and M. Chelliah, 2006: Leading tropical modes associated with interannual and multi-decadal fluctuations in North Atlantic hurricane activity. *J. Climate*, **19**, 590–612, https://doi.org/10.1175/JCLI3659.1.

——, and Coauthors, 2000: The 1999 North Atlantic Hurricane season [in "Climate Assessment for 1999"]. *Bull. Amer. Meteor. Soc.*, **81** (6), S19–S22, https://doi.org/10.1175/1520-0477(2000)81[s1:CAF]2.0.CO;2.

——, E. Blake, C. Landsea, K. Mo, R. Pasch, M. Chelliah, and S. Goldenberg, 2006: Atlantic basin [in "State of the Climate in 2005"]. *Bull. Amer. Meteor. Soc.*, **87** (6), S33–S37, https://doi.org/10.1175/1520-0477-87.6.S1.

——, ——, C. W. Landsea, C. Wang, J. Schemm, T. Kimberlain, R. J. Pasch, and S. B. Goldenberg, 2017: Atlantic basin [in "State of the Climate in 2016"]. *Bull. Amer. Meteor. Soc.*, **98** (8), S108–S112, https://doi.org/10.1175/2017BAMSStateoftheClimate.1.

——, ——, ——, S. B. Goldenberg, and R. J. Pasch, 2018: Atlantic basin [in "State of the Climate in 2017"]. *Bull. Amer. Meteor. Soc.*, **99** (8), S114–S118, https://doi.org/10.1175/2018BAMSStateoftheClimate.1.

——, ——, ——, H. Wang, S. B. Goldenberg, and R. J. Pasch 2019: Atlantic basin [in "State of the Climate in 2018"]. *Bull. Amer. Meteor. Soc.*, **100** (9), S113–S119, https://doi.org/10.1175/2019BAMSStateoftheClimate.1.

——, E. S. Blake, C. W. Landsea, M. Rosencrans, H. Wang, S. B. Goldenberg, and R. J. Pasch, 2020: Atlantic basin [in "State of the Climate in 2019"]. *Bull. Amer. Meteor. Soc.*, **101** (7), S204–S212, https://doi.org/10.1175/BAMS-D-20-0077.1.

Berg, R., 2024: Tropical cyclone report: Tropical Storm Max (EP162023). NHC NHC Tropical Cyclone Rep., 20 pp., https://www.nhc.noaa.gov/data/tcr/EP162023_Max.pdf.

Bjerknes, J., 1969: Atmospheric teleconnections from the equatorial Pacific. *Mon. Wea. Rev.*, **97**, 163–172, https://doi.org/10.1175/1520-0493(1969)097<0163:ATFTEP>2.3.CO;2.

Blake, E. S., 2024: Tropical cyclone report: Hurricane Beatriz (EP022023). NHC Tropical Cyclone Rep., 17 pp., https://www.nhc.noaa.gov/data/tcr/EP022023_Beatriz.pdf.

Camargo, S. J., and A. H. Sobel, 2005: Western North Pacific tropical cyclone intensity and ENSO. *J. Climate*, **18**, 2996–3006, https://doi.org/10.1175/JCLI3457.1.

——, A. W. Robertson, S. J. Gaffney, P. Smyth, and M. Ghil, 2007a: Cluster analysis of typhoon tracks: Part II: Large-scale circulation and ENSO. J. Climate, **20**, 3654–3676, https://doi.org/10.1175/JCLI4203.1.

——, K. A. Emanuel, and A. H. Sobel, 2007b: Use of a genesis potential index to diagnose ENSO effects on tropical cyclone genesis. *J. Climate*, **20**, 4819–4834, https://doi.org/10.1175/JCLI4282.1.

Chan, J. C. L., and K. S. Liu, 2002: Recent decrease in the difference in tropical cyclone occurrence between the Atlantic and the western North Pacific. *Adv. Atmos. Sci.*, **39**, 1387–1397.

Chen, L., and J.-J. Luo, 2021: Indian Ocean dipole and unique Indian Ocean basin warming in 2020 [in "State of the climate in 2020"]. *Bull. Amer. Meteor. Soc.*, **102** (8), S220–S222, https://doi.org/10.1175/BAMS-D-21-0080.1.

——, and ——, 2022: Indian Ocean dipole [in "State of the Climate in 2021"]. *Bull. Amer. Meteor. Soc.*, **103** (8), S213–S217, https://doi.org/10.1175/BAMS-D-22-0069.1.

Chia, H. H., and C. F. Ropelewski, 2002: The interannual variability in the genesis location of tropical cyclones in the northwest Pacific. *J. Climate*, **15**, 2934–2944, https://doi.org/10.1175/1520-0442(2002)015<2934:TIVITG>2.0.CO;2.

Courtney, J., and Coauthors, 2012: Documentation and verification of the world extreme wind gust record: 113.3 m s^{-1} on Barrow Island, Australia, during passage of tropical cyclone Olivia. *Aust. Meteor. Oceanogr. J.*, **62**, 1–9, https://doi.org/10.22499/2.6201.001.

Crosti, C., D. Duthinh, and E. Simiu, 2011: Risk consistency and synergy in multihazard design. *J. Struct. Eng.*, **137**, 844–849, https://doi.org/10.1061/(ASCE)ST.1943-541X.0000335.

Dare, R. A., and J. L. McBride, 2011: Sea surface temperature response to tropical cyclones. *Mon. Wea. Rev.*, **139**, 3798–3808, https://doi.org/10.1175/MWR-D-10-05019.1.

Diamond, H. J.,, and C. J. Schreck III, Eds., 2022: The tropics [in "State of the Climate in 2021"]. *Bull. Amer. Meteor. Soc.*, **103** (8), S193–S256, https://doi.org/10.1175/BAMS-D-22-0069.1.

——, and ——, Eds., 2023: The tropics [in "State of the Climate in 2022"]. *Bull. Amer. Meteor. Soc.*, **104** (8), S207–S270, https://doi.org/10.1175/BAMS-D-23-0078.1.

——, A. M. Lorrey, K. R. Knapp, and D. H. Levinson, 2012: Development of an enhanced tropical cyclone tracks database for the Southwest Pacific from 1840 to 2011. *Int. J. Climatol.*, **32**, 2240–2250, https://doi.org/10.1002/joc.2412.

Ding, Q., E. J. Steig, D. S. Battisti, and J. M. Wallace, 2012: Influence of the tropics on the southern annular mode. *J. Climate*, **25**, 6330–6348, https://doi.org/10.1175/JCLI-D-11-00523.1.

Domingues, R., and Coauthors, 2015: Upper ocean response to Hurricane Gonzalo (2014): Salinity effects revealed by targeted and sustained underwater glider observations. *Geophys. Res. Lett.*, **42**, 7131–7138, https://doi.org/10.1002/2015GL065378.

Dube, S. K., D. Rao, P. C. Sinha, T. S. Murty, and N. Bahuluyan, 1997: Storm surge in the Bay of Bengal and Arabian Sea: The problem and its prediction. *Mausam*, **48**, 283–304, https://doi.org/10.54302/mausam.v48i2.4012.

Earl-Spurr, C., and Coauthors, 2024: New WMO certified tropical cyclone duration extreme: TC Freddy (04 February to 14 March 2023) lasting for 36 days. *Bull. Amer. Meteor. Soc.*, in press, https://doi.org/10.1175/BAMS-D-24-0071.1.

Ebita, A., and Coauthors, 2011: The Japanese 55-Year Reanalysis "JRA-55": An interim report. *SOLA*, **7**, 149–152, https://doi.org/10.2151/sola.2011-038.

Emanuel, K. A., 1988: The maximum intensity of hurricanes. *J. Atmos. Sci.*, **45**, 1143–1155, https://doi.org/10.1175/1520-0469(1988)045<1143:TMIOH>2.0.CO;2.

—— , and D. S. Nolan, 2004: Tropical cyclone activity and the global climate system. 26th Conf. on Hurricanes and Tropical Meteorology, Miami, FL, Amer. Meteor. Soc., 10A.2, https://ams.confex.com/ams/26HURR/techprogram/paper_75463.htm.

Enfield, D. B., and A. M. Mestas-Nuñez, 1999: Multiscale variabilities in global sea surface temperatures and their relationships with tropospheric climate patterns. *J. Climate*, **12**, 2719–2733, https://doi.org/10.1175/1520-0442(1999)012<2719:MVIGSS>2.0.CO;2.

Franklin, J. L., M. L. Black, and K. Valde, 2003: GPS dropwindsonde wind profiles in hurricanes and their operational implications. *Wea. Forecasting*, **18**, 32–44, https://doi.org/10.1175/1520-0434(2003)018<0032:GDWPIH>2.0.CO;2.

Gallagher Re, 2024: Natural Catastrophe and Climate Report: 2023. 76 pp., https://www.ajg.com/gallagherre/news-and-insights/2024/january/2023-natural-catastrophe-and-climate-report/.

Goldenberg, S. B., and L. J. Shapiro, 1996: Physical mechanisms for the association of El Niño and West African rainfall with Atlantic major hurricane activity. *J. Climate*, **9**, 1169–1187, https://doi.org/10.1175/1520-0442(1996)009<1169:PMFTAO>2.0.CO;2.

—— , C. W. Landsea, A. M. Mestas-Nuñez, and W. M. Gray, 2001: The recent increase in Atlantic hurricane activity: Causes and implications. *Science*, **293**, 474–479, https://doi.org/10.1126/science.1060040.

Goni, G. J., and Coauthors, 2009: Applications of satellite-derived ocean measurements to tropical cyclone intensity forecasting. *Oceanography*, **22** (3), 190–197, https://doi.org/10.5670/oceanog.2009.78.

—— , and Coauthors, 2017: Autonomous and Lagrangian ocean observations for Atlantic tropical cyclone studies and forecasts. *Oceanography*, **30** (2), 92–103, https://doi.org/10.5670/oceanog.2017.227.

Gray, W. M., 1984: Atlantic seasonal hurricane frequency. Part I: El Niño and 30 mb quasi-biennial oscillation influences. *Mon. Wea. Rev.*, **112**, 1649–1668, https://doi.org/10.1175/1520-0493(1984)112<1649:ASHFPI>2.0.CO;2.

—— , 1990: Strong association between West African rainfall and U.S. landfall of intense hurricanes. *Science*, **249**, 1251–1256, https://doi.org/10.1126/science.249.4974.1251.

Guo, Y., X. Jiang, and D. E. Waliser, 2014: Modulation of the convectively coupled Kelvin waves over South America and the tropical Atlantic Ocean in association with the Madden–Julian oscillation. *J. Atmos. Sci.*, **71**, 1371–1388, https://doi.org/10.1175/JAS-D-13-0215.1.

Hastenrath, S., 1990: Decadal-scale changes of the circulation in the tropical Atlantic sector associated with Sahel drought. *Int. J. Climatol.*, **10**, 459–472, https://doi.org/10.1002/joc.3370100504.

Hersbach, H., and Coauthors, 2020: The ERA5 global reanalysis. *Quart. J. Roy. Meteor. Soc.*, **146**, 1999–2049, https://doi.org/10.1002/qj.3803.

Hong, C.-C., T. Li, and J.-J. Luo, 2008: Asymmetry of the Indian Ocean dipole. Part II: Model diagnosis. *J. Climate*, **21**, 4849–4858, https://doi.org/10.1175/2008JCLI2223.1.

Huang, B., and Coauthors, 2017: Extended Reconstructed Sea Surface Temperature, version 5 (ERSSTv5): Upgrades, validations, and intercomparisons. *J. Climate*, **30**, 8179–8205, https://doi.org/10.1175/JCLI-D-16-0836.1.

—— , C. Liu, V. Banzon, E. Freeman, G. Graham, B. Hankins, T. Smith, and H.-M. Zhang, 2021: Improvements of the Daily Optimum Interpolation Sea Surface Temperature (DOISST) version 2.1. *J. Climate*, **34**, 2923–2939, https://doi.org/10.1175/JCLI-D-20-0166.1.

Huffman, G., R. F. Adler, D. T. Bolvin, and G. Gu, 2009: Improving the global precipitation record: GPCP version 2.1. *Geophys. Res. Lett.*, **36**, L17808, https://doi.org/10.1029/2009GL040000.

Joyce, R. J., J. E. Janowiak, P. A. Arkin, and P. Xie, 2004: CMORPH: A method that produces global precipitation estimates from passive microwave and infrared data at high spatial and temporal resolution. *J. Hydrometeor.*, **5**, 487–503, https://doi.org/10.1175/1525-7541(2004)005<0487:CAMTPG>2.0.CO;2.

Kalnay, E., and Coauthors, 1996: The NCEP/NCAR 40-Year Reanalysis Project. *Bull. Amer. Meteor. Soc.*, **77**, 437–471, https://doi.org/10.1175/1520-0477(1996)077<0437:TNYRP>2.0.CO;2.

Kiladis, G. N., M. C. Wheeler, P. T. Haertel, K. H. Straub, and P. E. Roundy, 2009: Convectively coupled equatorial waves. *Rev. Geophys.*, **47**, RG2003, https://doi.org/10.1029/2008RG000266.

Knaff, J. A., 1997: Implications of summertime sea level pressure anomalies in the tropical Atlantic region. *J. Climate*, **10**, 789–804, https://doi.org/10.1175/1520-0442(1997)010<0789:IOSSLP>2.0.CO;2.

—— , C. R. Sampson, and K. D. Musgrave, 2018: An operational rapid intensification prediction aid for the western North Pacific. *Wea. Forecasting*, **33**, 799–811, https://doi.org/10.1175/WAF-D-18-0012.1.

—— , —— , and B. R. Strahl, 2020: A tropical cyclone rapid intensification prediction aid for the Joint Typhoon Warning Center's areas of responsibility. *Wea. Forecasting*, **35**, 1173–1185, https://doi.org/10.1175/WAF-D-19-0228.1.

Knapp, K. R., M. C. Kruk, D. H. Levinson, H. J. Diamond, and C. J. Neumann, 2010: The International Best Track Archive for Climate Stewardship (IBTrACS): Unifying tropical cyclone data. *Bull. Amer. Meteor. Soc.*, **91**, 363–376, https://doi.org/10.1175/2009BAMS2755.1.

—— , J. A. Knaff, C. R. Sampson, G. M. Riggio, and A. D. Schnapp, 2013: A pressure-based analysis of the historical western North Pacific tropical cyclone intensity record. *Mon. Wea. Rev.*, **141**, 2611–2631, https://doi.org/10.1175/MWR-D-12-00323.1.

Kumar, A., and Z.-Z. Hu, 2014: Interannual and interdecadal variability of ocean temperature along the equatorial Pacific in conjunction with ENSO. *Climate Dyn.*, **42**, 1243–1258, https://doi.org/10.1007/s00382-013-1721-0.

Landsea, C. W., and J. L. Franklin, 2013: Atlantic hurricane database uncertainty and presentation of a new database format. *Mon. Wea. Rev.*, **141**, 3576–3592, https://doi.org/10.1175/MWR-D-12-00254.1.

—— , W. M. Gray, P. W. Mielke, and K. J. Berry, 1992: Long-term variations of western Sahelian monsoon rainfall and intense U.S. landfalling hurricanes. *J. Climate*, **5**, 1528–1534, https://doi.org/10.1175/1520-0442(1992)005<1528:LTVOWS>2.0.CO;2.

—— , G. A. Vecchi, L. Bengtsson, and T. R. Knutson, 2010: Impact of duration thresholds on Atlantic tropical cyclone counts. *J. Climate*, **23**, 2508–2519, https://doi.org/10.1175/2009JCLI3034.1.

Leipper, D. F., and D. Volgenau, 1972: Hurricane heat potential of the Gulf of Mexico. *J. Phys. Oceanogr.*, **2**, 218–224, https://doi.org/10.1175/1520-0485(1972)002<0218:HHPOTG>2.0.CO;2.

Liebmann, B., and C. A. Smith, 1996: Description of a complete (interpolated) outgoing longwave radiation dataset. *Bull. Amer. Meteor. Soc.*, **77**, 1275–1277, https://doi.org/10.1175/1520-0477-77.6.1274.

Lin, I. I., and Coauthors, 2013: An ocean coupling potential intensity index for tropical cyclones. *Geophys. Res. Lett.*, **40**, 1878–1882, https://doi.org/10.1002/grl.50091.

—— , and Coauthors, 2020: ENSO and tropical cyclones. *El Niño Southern Oscillation in a Changing Climate, Geophys. Monogr.*, Vol. 253, Amer. Geophys. Union, 377–408, https://doi.org/10.1002/9781119548164.ch17.

—— , and Coauthors, 2021: A tale of two rapidly-intensifying supertyphoons: Hagibis (2019) and Haiyan (2013). Bull. *Amer. Meteor. Soc.*, **102**, E1645–E1664, https://doi.org/10.1175/BAMS-D-20-0223.1.

Liu, T., J. Li, C. Sun, T. Lian, and Y. Zhang, 2021: Impact of the April–May SAM on central Pacific Ocean sea temperature over the following three seasons. *Climate Dyn.*, **57**, 775–786, https://doi.org/10.1007/s00382-021-05738-4.

—— , S. Masson, S. Behera, and T. Yamagata, 2007: Experimental forecasts of the Indian Ocean dipole using a coupled OAGCM. *J. Climate*, **20**, 2178–2190, https://doi.org/10.1175/JCLI4132.1.

—— , R. Zhang, S. K. Behera, Y. Masumoto, F.-F. Jin, R. Lukas, and T. Yamagata, 2010: Interaction between El Niño and extreme Indian Ocean dipole. *J. Climate*, **23**, 726–742, https://doi.org/10.1175/2009JCLI3104.1.

—— , W. Sasaki, and Y. Masumoto, 2012: Indian Ocean warming modulates Pacific climate change. *Proc. Natl. Acad. Sci. USA*, **109**, 18 701–18 706, https://doi.org/10.1073/pnas.1210239109.

Madden, R., and P. Julian, 1971: Detection of a 40–50 day oscillation in the zonal wind in the tropical Pacific. *J. Atmos. Sci.*, **28**, 702–708, https://doi.org/10.1175/1520-0469(1971)028<0702:DOADOI>2.0.CO;2.

—— , and —— , 1972: Description of global-scale circulation cells in the tropics with a 40–50 day period. *J. Atmos. Sci.*, **29**, 1109–1123, https://doi.org/10.1175/1520-0469(1972)029<1109:DOGSCC>2.0.CO;2.

—— , and —— , 1994: Observations of the 40–50-day tropical oscillation: A review. *Mon. Wea. Rev.*, **122**, 814–837, https://doi.org/10.1175/1520-0493(1994)122<0814:OOTDTO>2.0.CO;2.

Mainelli, M., M. DeMaria, L. Shay, and G. Goni, 2008: Application of oceanic heat content estimation to operational forecasting of recent Atlantic category 5 hurricanes. *Wea. Forecasting*, **23**, 3–16, https://doi.org/10.1175/2007WAF2006111.1.

Maloney, E. D., and D. L. Hartmann, 2001: The Madden–Julian oscillation, barotropic dynamics, and North Pacific tropical cyclone formation. *Part I: Observations. J. Atmos. Sci.*, **58**, 2545–2558, https://doi.org/10.1175/1520-0469(2001)058<2545:TMJOBD>2.0.CO;2.

Menne, M. J., B. E. Gleason, J. Lawrimore, J. Rennie, and C. N. Williams, 2017: Global Historical Climatology Network – Monthly temperature, version 4 (BETA). NOAA National Centers for Environmental Information, accessed 31 January 2024, https://doi.org/10.7289/V5XW4GTH.

Moreno, P. I., and Coauthors, 2018: Onset and evolution of southern annular mode-like changes at centennial timescale. *Sci. Rep.*, **8**, 3458, https://doi.org/10.1038/s41598-018-21836-6.

Münnich, M., and J. D. Neelin, 2005: Seasonal influence of ENSO on the Atlantic ITCZ and equatorial South America. *Geophys. Res. Lett.*, **32**, L21709, https://doi.org/10.1029/2005GL023900.

NIWA, 2023: Aotearoa New Zealand climate summary: February 2023 (issued 3 March 2023). Accessed 2 February 2024, https://niwa.co.nz/monthly/climate-summary-february-2023.

NOAA, 2023: Climate diagnostics bulletin, September 2023. NOAA, 87 pp., https://www.cpc.ncep.noaa.gov/products/CDB/CDB_Archive_pdf/PDF/CDB.sep2023_color.pdf.

Nobre, P., and J. Shukla, 1996: Variations of sea surface temperature, wind stress and rainfall over the tropical Atlantic and South America. *J. Climate*, **9**, 2464–2479, https://doi.org/10.1175/1520-0442(1996)009<2464:VOSSTW>2.0.CO;2.

Parvez, C. (@ChaudharyParvez), 2023: Residential building in Acapulco, Mexico that was shredded by Category 5 Hurricane Otis's extreme winds. Twitter/X, 28 October 2023, 10:40 p.m., https://twitter.com/ChaudharyParvez/status/1718457833468125236.

Raga, G. B., B. Bracamontes-Ceballos, L. Farfán, and R. Romero-Centeno, 2013: Landfalling tropical cyclones on the Pacific coast of Mexico: 1850–2010. *Atmósfera*, **26**, 209–220, https://doi.org/10.1016/S0187-6236(13)71072-5.

Ramage, C. S., 1971: *Monsoon Meteorology*. Academic Press, 296 pp.

Reinhart, B. J., and A. Reinhart, 2024: Hurricane Otis (EP182023). NHC Tropical Cyclone Rep., 39 pp., https://www.nhc.noaa.gov/data/tcr/EP182023_Otis.pdf.

Reynolds, R. W., N. A. Rayner, T. M. Smith, D. C. Stokes, and W. Wang, 2002: An improved in situ and satellite SST analysis for climate. *J. Climate*, **15**, 1609–1625, https://doi.org/10.1175/1520-0442(2002)015<1609:AIISAS>2.0.CO;2.

Ropelewski, C. F., and M. S. Halpert, 1989: Precipitation patterns associated with the high index phase of the Southern Oscillation. *J. Climate*, **2**, 268–284, https://doi.org/10.1175/1520-0442(1989)002<0268:PPAWTH>2.0.CO;2.

Saha, S., and Coauthors, 2014: The NCEP Climate Forecast System version 2. *J. Climate*, **27**, 2185–2208, https://doi.org/10.1175/JCLI-D-12-00823.1.

Saji, N. H., B. N. Goswami, P. N. Vinayachandran, and T. Yamagata, 1999: A dipole mode in the tropical Indian Ocean. *Nature*, **401**, 360–363, https://doi.org/10.1038/43854.

Schneider, T., T. Bischoff, and G. H. Haug, 2014: Migrations and dynamics of the intertropical convergence zone. *Nature*, **513**, 45–53, https://doi.org/10.1038/nature13636.

Schreck, C. J., 2015: Kelvin waves and tropical cyclogenesis: A global survey. *Mon. Wea. Rev.*, **143**, 3996–4011, https://doi.org/10.1175/MWR-D-15-0111.1.

—— , 2016: Convectively coupled Kelvin waves and tropical cyclogenesis in a semi-Lagrangian framework. *Mon. Wea. Rev.*, **144**, 4131–4139, https://doi.org/10.1175/MWR-D-16-0237.1.

—— , and J. Molinari, 2011: Tropical cyclogenesis associated with Kelvin waves and the Madden–Julian oscillation. *Mon. Wea. Rev.*, **139**, 2723–2734, https://doi.org/10.1175/MWR-D-10-05060.1.

—— , K. R. Knapp, and J. P. Kossin, 2014: The impact of best track discrepancies on global tropical cyclone climatologies using IBTrACS. Mon. *Wea. Rev.*, **142**, 3881–3899, https://doi.org/10.1175/MWR-D-14-00021.1.

—— , H.-T. Lee, and K. R. Knapp, 2018: HIRS outgoing longwave radiation —— Daily climate data record: Application toward identifying tropical subseasonal variability. *Remote Sens.*, **10**, 1325, https://doi.org/10.3390/rs10091325.

Shay, L. K., G. J. Goni, and P. G. Black, 2000: Effects of a warm oceanic feature on Hurricane Opal. *Mon. Wea. Rev.*, **128**, 1366–1383, https://doi.org/10.1175/1520-0493(2000)128<1366:EOAWOF>2.0.CO;2.

Trenberth, K. E., 1984: Signal versus noise in the Southern Oscillation. *Mon. Wea. Rev.*, **112**, 326–332, https://doi.org/10.1175/1520-0493(1984)1122.0.CO;2.

Vecchi, G. A., and B. J. Soden, 2007: Effect of remote sea surface temperature change on tropical cyclone potential intensity. *Nature*, **450**, 1066–1070, https://doi.org/10.1038/nature06423.

Ventrice, M. J., C. D. Thorncroft, and M. A. Janiga, 2012a: Atlantic tropical cyclogenesis: A three-way interaction between an African easterly wave, diurnally varying convection, and a convectively coupled atmospheric Kelvin wave. *Mon. Wea. Rev.*, **140**, 1108–1124, https://doi.org/10.1175/MWR-D-11-00122.1.

—— , —— , and C. J. Schreck, 2012b: Impacts of convectively coupled Kelvin waves on environmental conditions for Atlantic tropical cyclogenesis. *Mon. Wea. Rev.*, **140**, 2198–2214, https://doi.org/10.1175/MWR-D-11-00305.1.

Villarini, G., G. A. Vecchi, T. R. Knutson, and J. A. Smith, 2011: Is the recorded increase in short duration North Atlantic tropical storms spurious? *J. Geophys. Res.*, **116**, D10114, https://doi.org/10.1029/2010JD015493.

Vincent, D. G., 1994: The South Pacific Convergence Zone (SPCZ): A review. *Mon. Wea. Rev.*, **122**, 1949–1970, https://doi.org/10.1175/1520-0493(1994)122<1949:TSPCZA>2.0.CO;2.

Vose, R. S., and Coauthors, 2021: Implementing full spatial coverage in NOAA's Global Temperature Analysis. *Geophys. Res. Lett.*, **48**, e2020GL090873, https://doi.org/10.1029/2020GL090873.

Waliser, D. E., and C. Gautier, 1993: A satellite-derived climatology of the ITCZ. *J. Climate*, **6**, 2162–2174, https://doi.org/10.1175/1520-0442(1993)006<2162:ASDCOT>2.0.CO;2.

Wang, B., 1994: Climatic regimes of tropical convection and rainfall. *J. Climate*, **7**, 1109–1118, https://doi.org/10.1175/1520-0442(1994)007<1109:CROTCA>2.0.CO;2.

—— , and Q. Ding, 2008: Global monsoon: Dominant mode of annual variation in the tropics. *Dyn. Atmos. Ocean*, **44**, 165–183, https://doi.org/10.1016/j.dynatmoce.2007.05.002.

—— , J. Liu, H. J. Kim, P. J. Webster, and S. Y. Yim, 2012: Recent change of the global monsoon precipitation (1979–2008). *Climate Dyn.*, **39**, 1123–1135, https://doi.org/10.1007/s00382-011-1266-z.

Wheeler, M., and G. N. Kiladis, 1999: Convectively coupled equatorial waves: Analysis of clouds and temperature in the wavenumber-frequency domain. *J. Atmos. Sci.*, **56**, 374–399, https://doi.org/10.1175/1520-0469(1999)056<0374:CCEWAO>2.0.CO;2.

Wheeler, M. C., and H. H. Hendon, 2004: An all-season real-time multivariate MJO index: Development of an index for monitoring and prediction. *Mon. Wea. Rev.*, **132**, 1917–1932, https://doi.org/10.1175/1520-0493(2004)132<1917:AARMMI>2.0.CO;2.

Wood, K. M., and E. A. Ritchie, 2015: A definition for rapid weakening in the North Atlantic and eastern North Pacific. *Geophys. Res. Lett.*, **42**, 10 091–10 097, https://doi.org/10.1002/2015GL066697.

—— , and C. J. Schreck, 2020: Eastern North Pacific and central North Pacific basins [in "State of the Climate in 2019"]. *Bull. Amer. Meteor. Soc.*, **101** (8), S212–S214, https://doi.org/10.1175/BAMS-D-20-0077.1.

—— , and —— , 2021: Eastern North Pacific and central North Pacific basins [in "State of the Climate in 2020"]. *Bull. Amer. Meteor. Soc.*, **102** (8), S233–S235, https://doi.org/10.1175/BAMS-D-21-0080.1.

—— , and —— , 2022: Eastern North Pacific and central North Pacific basins [in "State of the Climate in 2021"]. *Bull. Amer. Meteor. Soc.*, **103** (8), S229–S231, https://doi.org/10.1175/BAMS-D-22-0069.1.

—— , and —— , 2023: Eastern North Pacific and central North Pacific basins [in "State of the Climate in 2022"]. *Bull. Amer. Meteor. Soc.*, **104** (8), S239–S243, https://doi.org/10.1175/BAMS-D-23-0078.1.

Wu, J., F. Hanjie, L. Shuheng, Z. Wenxiu, S. Yang, S. He, and N. Keenlyside, 2024: Boosting effect of strong western pole of the Indian Ocean dipole on the decay of El Niño events. *npj Climate Atmos. Sci.*, **7**, 6, https://doi.org/10.1038/s41612-023-00554-5.

Yim, S. Y., B. Wang, J. Liu, and Z. W. Wu, 2014: A comparison of regional monsoon variability using monsoon indices. *Climate Dyn.*, **43**, 1423–1437, https://doi.org/10.1007/s00382-013-1956-9.

Zhang, C., 2005: Madden–Julian oscillation. *Rev. Geophys.*, **43**, RG2003, https://doi.org/10.1029/2004RG000158.

Zhao, J. W., R. F. Zhan, Y. Q. Wang, and H. M. Xu, 2018: Contribution of the Interdecadal Pacific oscillation to the recent abrupt decrease in tropical cyclone genesis frequency over the western North Pacific since 1998. *J. Climate*, **31**, 8211–8224, https://doi.org/10.1175/JCLI-D-18-0202.1.

—— , —— , —— , S.-P. Xie, and Q. Wu, 2020: Untangling impacts of global warming and interdecadal Pacific Oscillation on long-term variability of North Pacific tropical cyclone track density. *Sci. Adv.*, **6**, eaba6813, https://doi.org/10.1126/sciadv.aba6813.

Zheng, Z.-W., I.-I. Lin, B. Wang, H.-C. Huang, and C.-H. Chen, 2015: A long neglected Rdamper in the El Nino–typhoon relationship: A 'Gaia-like' process. *Sci. Rep.*, **5**, 11103, https://doi.org/10.1038/srep11103.